



# A Spectroscopic Analysis of Clay Types and Silty Sand from Oltu/Erzurum (Turkey) Region Reinforcing with Marble Dust and Waste Tire

*Mermer Tozu ve Atık Lastikle Takviye Edilmiş Oltu/Erzurum (Türkiye) Bölgesine Ait Kil Türleri ve Siltli Kumun Spektroskopik Analizi*

Zeynep Aygun<sup>1\*</sup> , Necmi Yarbaşı<sup>2</sup> 

<sup>1</sup>Bitlis Eren University, Vocational School of Technical Sciences, Bitlis, Turkey

<sup>2</sup>Ataturk University, Oltu Earth Sciences Faculty, Geological Engineering Department, Erzurum, Turkey

## Abstract

In the present study, it has been aimed to give a comprehensive analysis of unreinforced and reinforced materials (with waste tire and marble dust additions in different amounts); clays (green and red) and silty sand, obtained from Oltu/Erzurum region which consists of Oligocene lower upper sedimentary units, volcanic rocks and upper sedimentary units. In order to investigate the magnetic properties of these samples, electron paramagnetic resonance has been used; to see the crystalline nature x-ray diffraction has been performed; to observe the surface morphology scanning electron microscope has been used and to learn the elemental compositions energy dispersive spectroscopy has been preferred.

**Keywords:** Clay, Magnetic properties, Reinforced materials, Silty sand

## Öz

Bu çalışmada, Oligosen yaşlı alt sedimanter birim, volkanik birim ve üst sedimanter birimden oluşan Oltu/Erzurum bölgesine ait takviye edilmemiş ve takviye edilmiş (atık lastik ve mermer tozunun farklı miktarlarda eklenmesi ile) kil türleri ve siltli kum örneklerinin kapsamlı bir analizinin verilmesi amaçlanmıştır. Bu örneklerin manyetik özelliklerini incelemek için elektron paramanyetik rezonans kullanılmıştır, kristal doğasını görmek için x-ışını kırınımı performe edilmiştir, yüzey morfolojisini gözlemlemek için taramalı elektron mikroskobu kullanılmış ve elementel kompozisyonu öğrenmek için enerji dağılımlı spektroskopi tercih edilmiştir.

**Anahtar Kelimeler:** Kil, Manyetik özellikler, Takviye edilmiş malzemeler, Siltli kum

## 1. Introduction

Recently, soil reinforcement used for improving the stability, increasing the resistance or bearing capacity of the construction material are widely experienced by researchers (Wei et al. 2015, Ghazavi and Roustaei 2010, Akbulut et al. 2007). Different kinds of soil materials; clayey soil and silty soil are studied in different ways previously. Soil properties have great importance not only for reinforcement properties but also for agricultural applications. It is well known that there is a correlation between soil type and fertility. Additions, marble dust or waste tire, chosen for reinforcing the soil materials obtained from different regions attracts

the attention of researchers (Kalkan and Bayraktutan 2008, Taşpolat et al. 2006, Altun et al. 2009, Jafari and Esna-ashari 2012). The clay soil by its geotechnical applications and engineering properties has been researched by Kalkan and Bayraktutan (2008). The addition of marble dust to clay layers has also been investigated by Taşpolat et al. (2006). Another material, silty soil with different contents has been studied by Altun et al. (2009). Also, reinforcing with a waste tire has been searched by Jafari and Esna-ashari (2012).

In the present study, our aim is to investigate the magnetic properties, structural features, compositions of these soil materials (clay types, silty sand, waste tire and marble dust). These clay and silty sand materials have the characteristics of Oltu/Erzurum region consisting of Oligocene lower upper sedimentary units, volcanic rocks and upper sedimentary units. The lower sedimentary unit consists of conglomerate,

\*Corresponding author: [zeynep.yarbasi@gmail.com](mailto:zeynep.yarbasi@gmail.com)

Zeynep Aygun  [orcid.org/0000-0002-2979-0283](https://orcid.org/0000-0002-2979-0283)

Necmi Yarbaşı  [orcid.org/0000-0003-4259-1278](https://orcid.org/0000-0003-4259-1278)

sandstone, silt-clay layers and gypsum-limestone band. The upper sedimentary unit has high clay content (Yarbaşı 2016). These regional properties will have important effects on both agricultural and reinforcement applications. In order to detect paramagnetic properties, we have used EPR (electron paramagnetic resonance) technique, that helps us to identify quantum systems with unpaired electron in the presence of an external magnetic field by using the microwave region of the electromagnetic spectrum. In the geological sciences, EPR is comparatively unrecognized while it has been applied in the fields of determinative mineralogy (Marfunin 1964). EPR is used as an instrumental tool in geology for the detection of certain ionic species in minerals and rocks. EPR also has advantages because of having an important property: less than 0.5 g of the sample (solid, liquid, or powder) required for analysis (Cubitt 1979). Additionally, we have carried out XRD (X-ray diffraction) study to make qualitative analysis of materials. XRD is a considerable method to get information about the crystallographic structure and chemical composition of any crystalline material. For surface morphology, we have used SEM (scanning electron microscope) method. Also, EDS (energy dispersive spectroscopy) has been preferred to see the elemental compositions. While reinforced materials (clay and silty sand) were studied many times before for different purposes as mentioned above, spectroscopic analysis of these regional materials have not been carried out. To our knowledge, magnetic and structural properties, crystalline nature of these regional unreinforced and reinforced materials have not been studied before. Therefore, a comprehensive analysis of these samples which is important both for agricultural applications and reinforcement features will be helpful to address this lack.

## 2. Experimental

### 2.1. Sample Preparation

In this study, clay and silty sand samples were obtained from Oligocene old sediments, 0.50 m depth from the surface, in the western part of Oltu (Erzurum). The clay floor brought to the laboratory environment was dried at  $105 \pm 5^\circ\text{C}$  for 24 hours. The cured granules were milled at 2000 cycles in the device Angeles. Waste tire fragments which constitute the second most important component of the work, were taken from Erzurum industry region. Obtained shredded waste tire pieces (1.18 mm, 2.00 mm and 3.15 mm) were shaken in the sieve machine. Marble dust was obtained from Afyon region by polishing, scraping and carving operations of the

marbles. In order to remove the coarse particles in the dry marble dust, 0.125 mm sieve was used.

### 2.2. Instrumentation

EPR experiments were performed at room temperature by using an X-band JEOL JESFA-300 EPR spectrometer with 100 kHz modulation field and 9.23 GHz frequency. The XRD patterns of alloy samples were recorded by JEOL D8 ADVANCE XRD spectrometer, which was operated at 40 kV and 40 mA with a scanning speed of  $2.5^\circ \text{min}^{-1}$ . Cu- $K\alpha$  radiation of wavelength  $\lambda = 1.54060 \text{ \AA}$  was used and data were taken for the  $2\theta$  range of  $20 - 80^\circ$ .

In SEM technique, an electron gun with thermoionic emission is usually used for producing electron. The signals composed as a result of the interaction between incident electron beam and sample give us different information about the specimen. The scanning electron microscope images of powders were measured by JEOL JSM-6610 SEM Spectrometer. Also, EDS analysis of the samples were performed.

## 3. Results and Discussion

### 3.1. EPR Analysis

The recorded EPR spectra for red and green clays, silty sand, waste tire, marble dust samples have been investigated at room temperature. The obtained  $g$ -factor of the EPR lines have been calculated from the equation

$$h\nu = g\beta H \quad (1)$$

with  $H$  the magnetic field,  $\nu$  the microwave frequency,  $h$  the planck constant and  $\beta$  the electron bohr magneton.

As seen in Figure 1A, EPR spectrum recorded for green clay has given two kinds of signals with  $g$  values of 4.392 and 2.013. The signal of  $g = 4.392$  has been attributed to iron center. The resonance at  $g \approx 4.3$  corresponds to high-spin isolated  $\text{Fe}^{+3}$  in the glassy matrix (Aygun and Aygun 2016). We have seen EPR lines with  $g = 2.013$  assigned as Mn ( $I = 5/2$ ) six hyperfine lines ( $g \approx 2.00$ ) (Yarbasi et al. 2011). We are also able to see the forbidden transition lines (five weak doublets) of Mn ( $\Delta m_1 = \pm 1$ ) between main six peaks (Bennur et al. 2001). In Figure 1B, for red clay two EPR signals have been obtained with  $g$  values of 4.388 and 2.00. These values have been assigned as Fe center and Mn sextet. For marble dust, we have observed Mn sextet with  $g = 2.012$  and forbidden transition lines (five weak doublets) given by Figure 1C. EPR spectrum given in Figure 1D has shown a singlet with  $g$  value of 2.002 defined as  $\text{Mn}^{4+}$

**Table 1.** g values ( $\pm 0.005$ ) obtained from EPR experiments.

Sample	Fe center	Mn <sup>2+</sup> center	Mn <sup>4+</sup>
Green clay	4.392	2.013	-
Red clay	4.388	2.000	-
Marble dust	-	2.012	-
Waste tire	-	-	2.002
Green clay with %5 marble dust and %0.5 waste tire	4.357	2.009	-
Red clay with %5 marble dust and %0.5 waste tire	4.382	2.009	-
Green clay with %5 marble dust	-	2.020	-
Red clay with %5 marble dust	4.385	2.032	-
Silty sand	4.355	2.008	-
Silty sand with %10 marble dust	4.356	2.020	-
Silty sand with %10 marble dust and %0.5 waste tire.	4.359	2.010	-

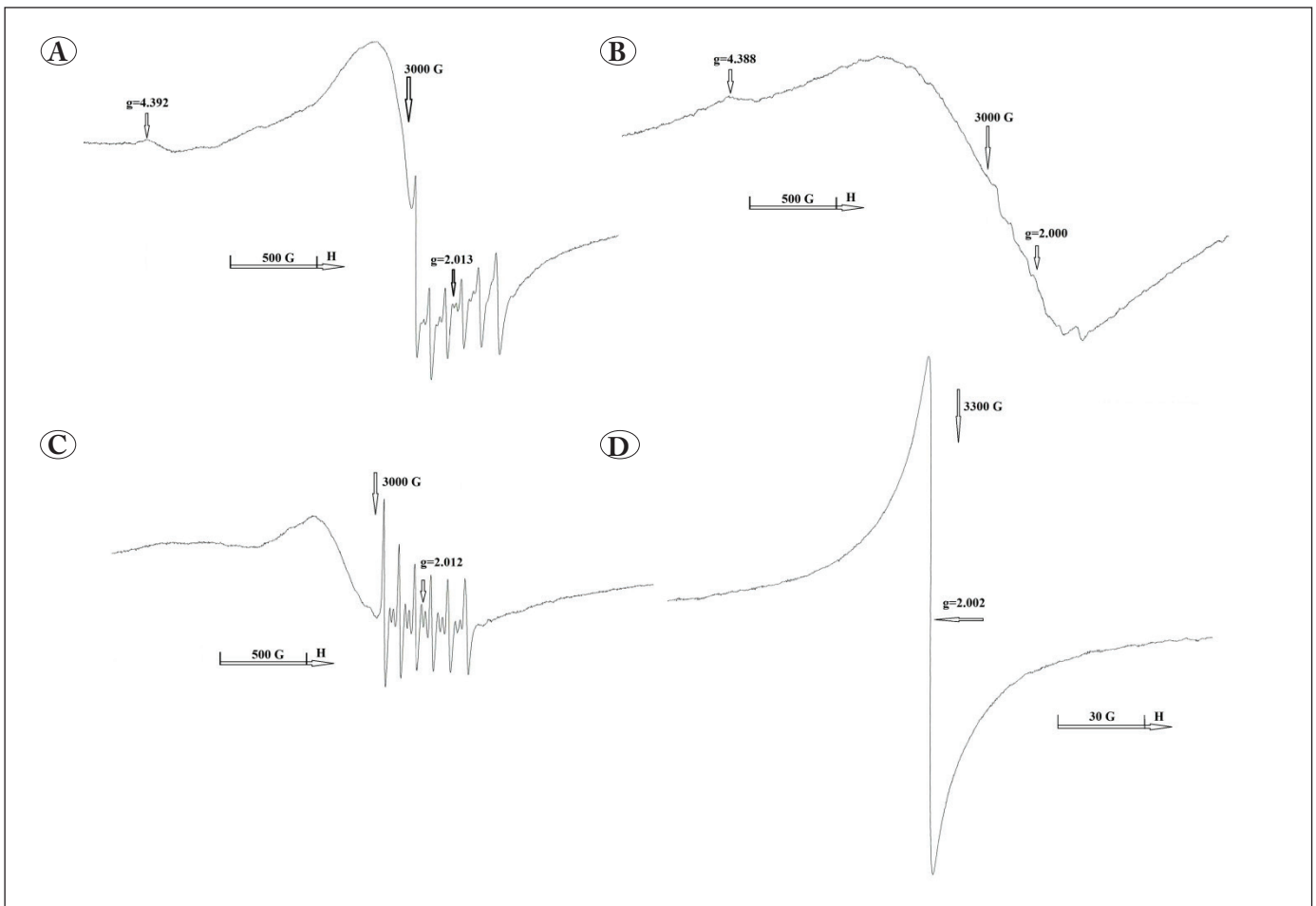


**Figure 1.** Room temperature EPR spectra of A) green clay B) red clay C) marble dust D) waste tire.

(Stoyanova et al. 2000). In Figure 2A, we have observed Mn sextet with  $g = 2.009$  and ferric center signal with  $g = 4.357$  for green clay with %5 marble dust and waste tire, but while Mn peaks with a  $g$  value of 2.020 have been seen, iron center has been vanished for green clay with only marble dust as shown in Figure 2C. For red clay sample with marble dust and waste tire/without waste tire have given signals with  $g = 4.382 / 4.385$  respectively (Figures 2B, D). In Figure 3, for silty sand samples with/without additives, EPR spectra have given both iron center and Mn six hyperfines. All these iron centers can be attributed to  $Fe^{+3}$  ion (Aygun and Aygun 2016).

### 3.2. XRD Analysis

As given by Figure 4, XRD study of green clay, red clay, marble dust and waste tire have been carried out at room temperature. For all samples, we are able to see the main ferric peaks assigned as  $Fe_3O_4$ ,  $Fe_2O_3$ ,  $FeAl$  or  $Fe$  with  $2\theta \approx 19^\circ, 20^\circ, 30^\circ, 35^\circ, 37^\circ, 39^\circ, 49^\circ, 63^\circ$  (Musolino 2010, Shu and Wang 2009, Senderowski 2014, Li et al. 2016). These centers are also observed in EPR spectra. In Figure 4, it is seen that Mn peaks located at  $\approx 29^\circ, 39.5^\circ, 43.5^\circ$  and  $57.5^\circ$  (Sun et al. 2013, Zhang et al. 2012) also given by EPR spectra. For all kinds of samples, we can observe silicon and

$SiO_2$  compositions centered at  $\approx 22.5^\circ, 29^\circ$  and  $48^\circ$  (Ferreira et al. 2015, Yang et al. 2009). In Figure 5A-D, we have seen given elemental and oxide peaks for green and red clays with marble dust, with and without waste tire. For silty sand and its doped forms have been given in Figure 6. Intense calcite peaks ( $\approx 29^\circ, 39^\circ, 43^\circ$ ) have been obtained from XRD patterns (Rahman et al. 2013). Except for silty sand with waste tire and marble dust, XRD spectra for all samples have showed Ti and  $TiO_2$  peaks centered at  $\approx 27^\circ, 36^\circ, 38^\circ, 40^\circ, 44^\circ, 48^\circ, 65^\circ$  (Fisli et al. 2017, Lu et al. 2011). All XRD peaks gives us chance to evaluate the samples in crystalline nature.

### 3.3. EDS Analysis

Room temperature EDS measurements of clays, silty sand, marble dust and waste tire have been carried out in order to determine the elemental compositions and obtained results are given in Figures 7-9. As seen from EDS results, the components with weight % of all samples are in good agreement with XRD and EPR results.

### 3.4. SEM Analysis

In SEM analysis, secondary electrons (SE, inelastic scattering) are used for determining sample morphology

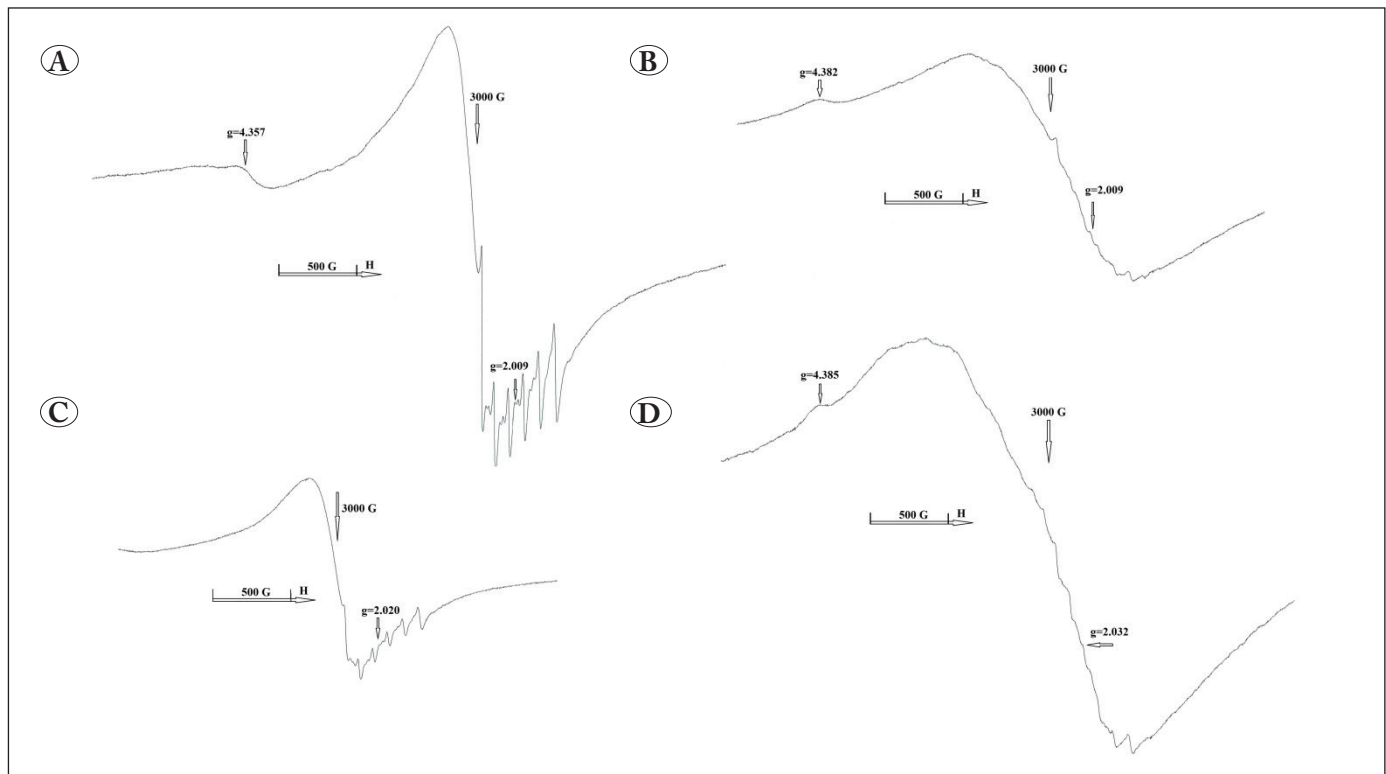


**Figure 2.** Room temperature EPR spectra of **A)** green clay with %5 marble dust and %0.5 waste tire **B)** red clay with %5 marble dust and %0.5 waste tire **C)** green clay with %5 marble dust **D)** red clay with %5 marble dust.

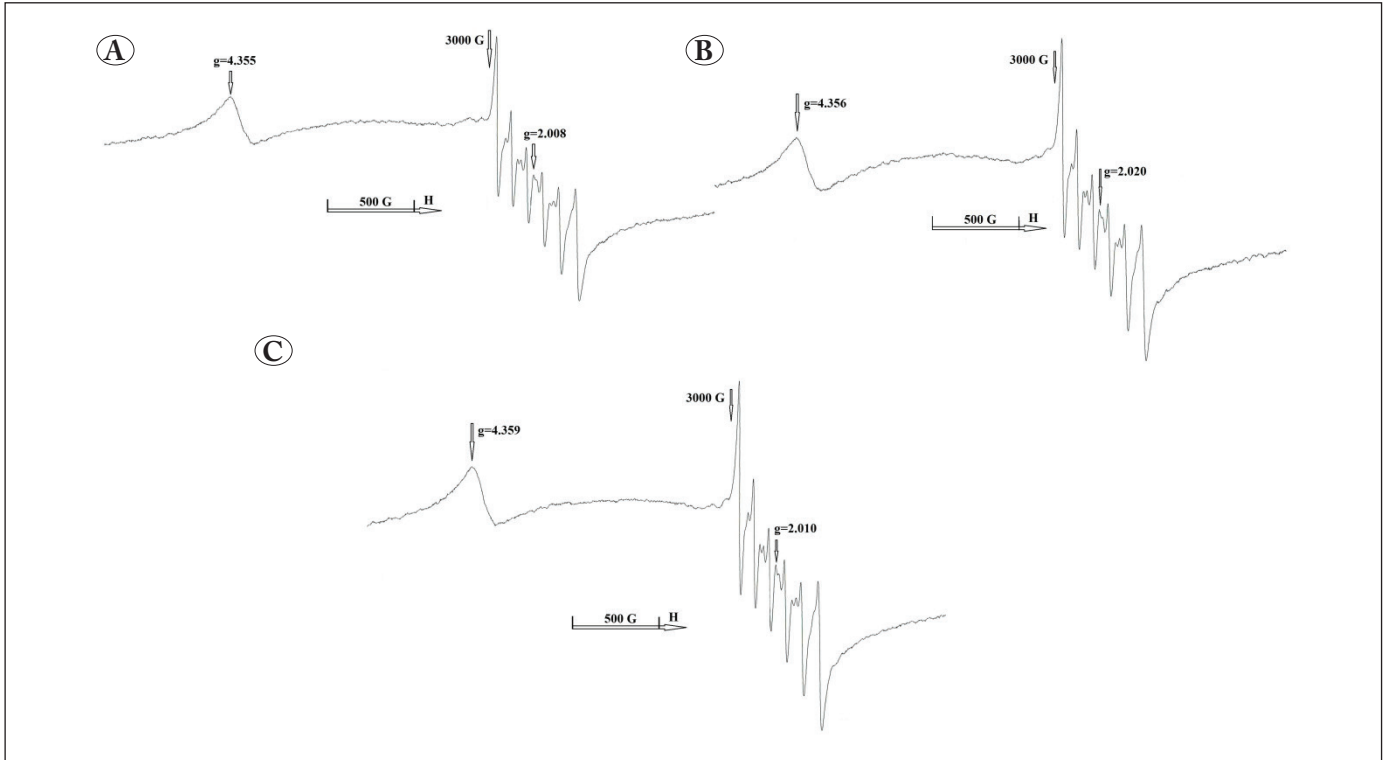


**Figure 3.** Room temperature EPR spectra of **A)** silty sand **B)** silty sand with %10 marble dust **C)** silty sand with %10 marble dust and %0.5 waste tire.

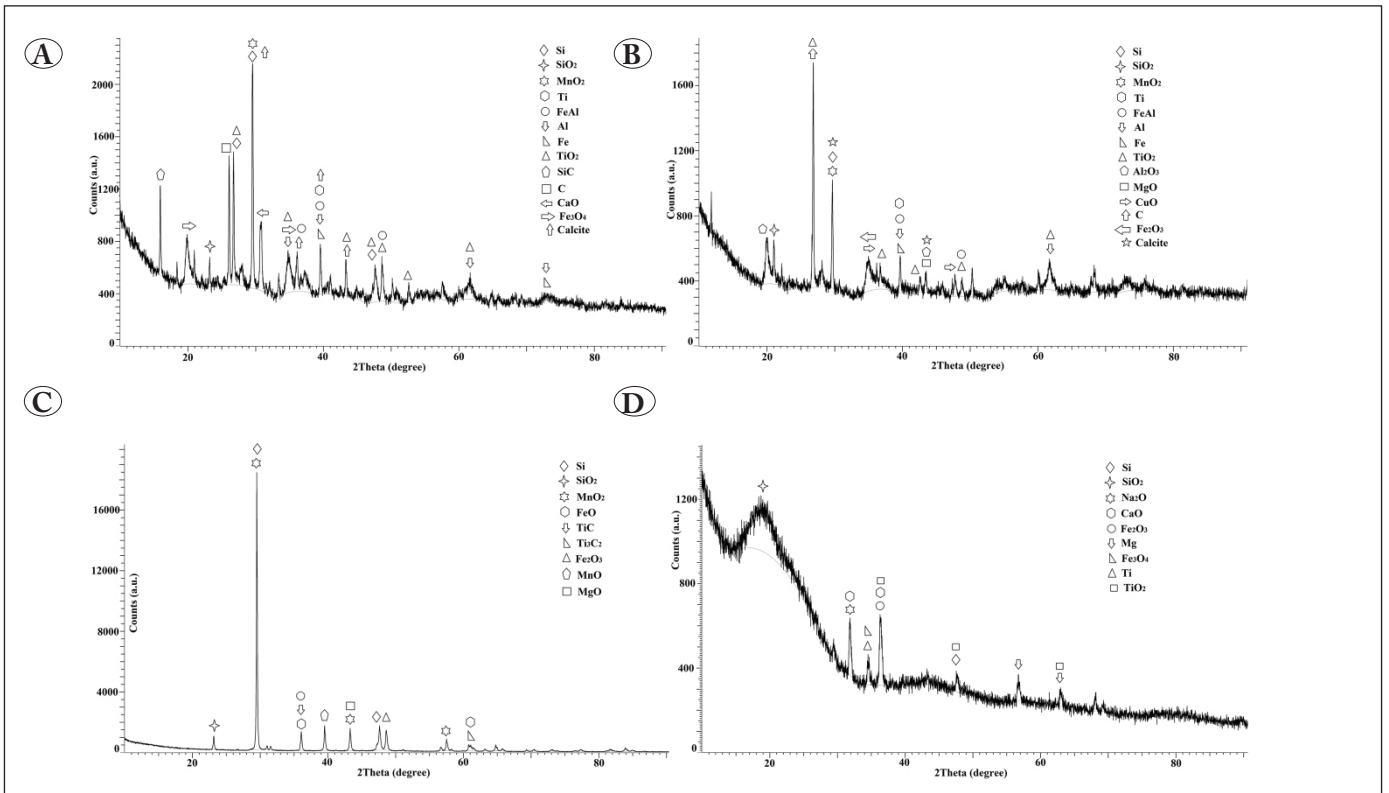


**Figure 4.** Room temperature XRD patterns of **A)** green clay **B)** red clay **C)** marble dust **D)** waste tire.

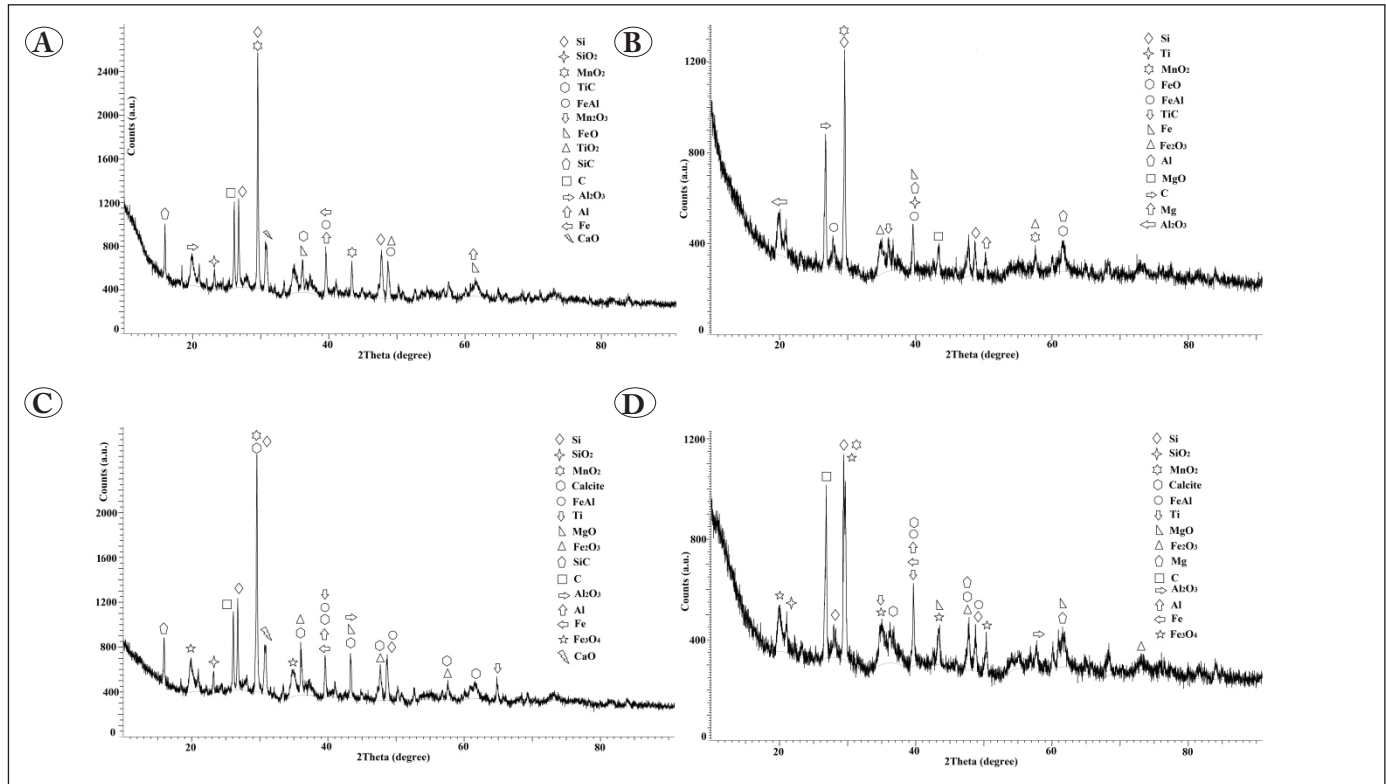


Figure 5. Room temperature XRD patterns of A) green clay with %5 marble dust and %0.5 waste tire B) red clay with %5 marble dust and %0.5 waste tire C) green clay with %5 marble dust D) red clay with %5 marble dust.

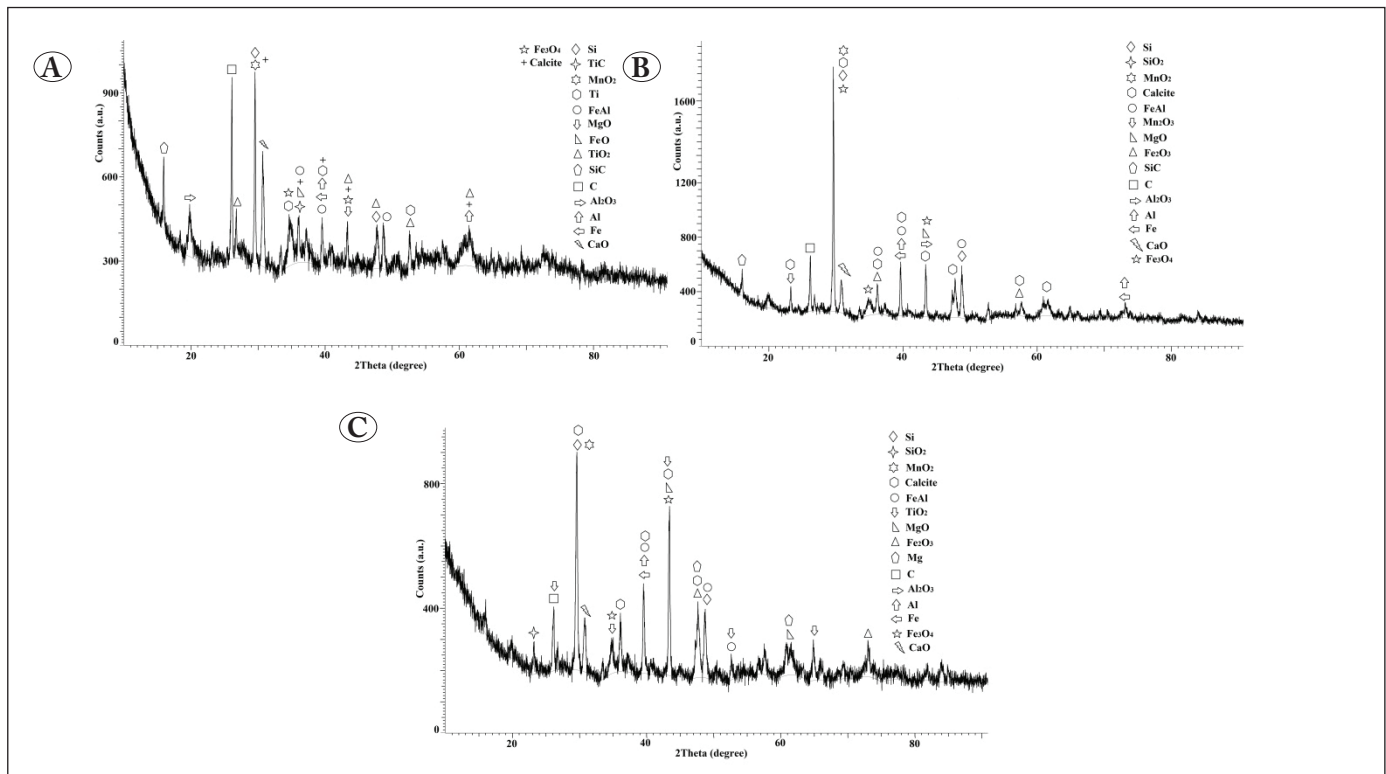


Figure 6. Room temperature XRD patterns A) silty sand B) silty sand with %10 marble dust and %0.5 waste tire C) silty sand with %10 marble dust.

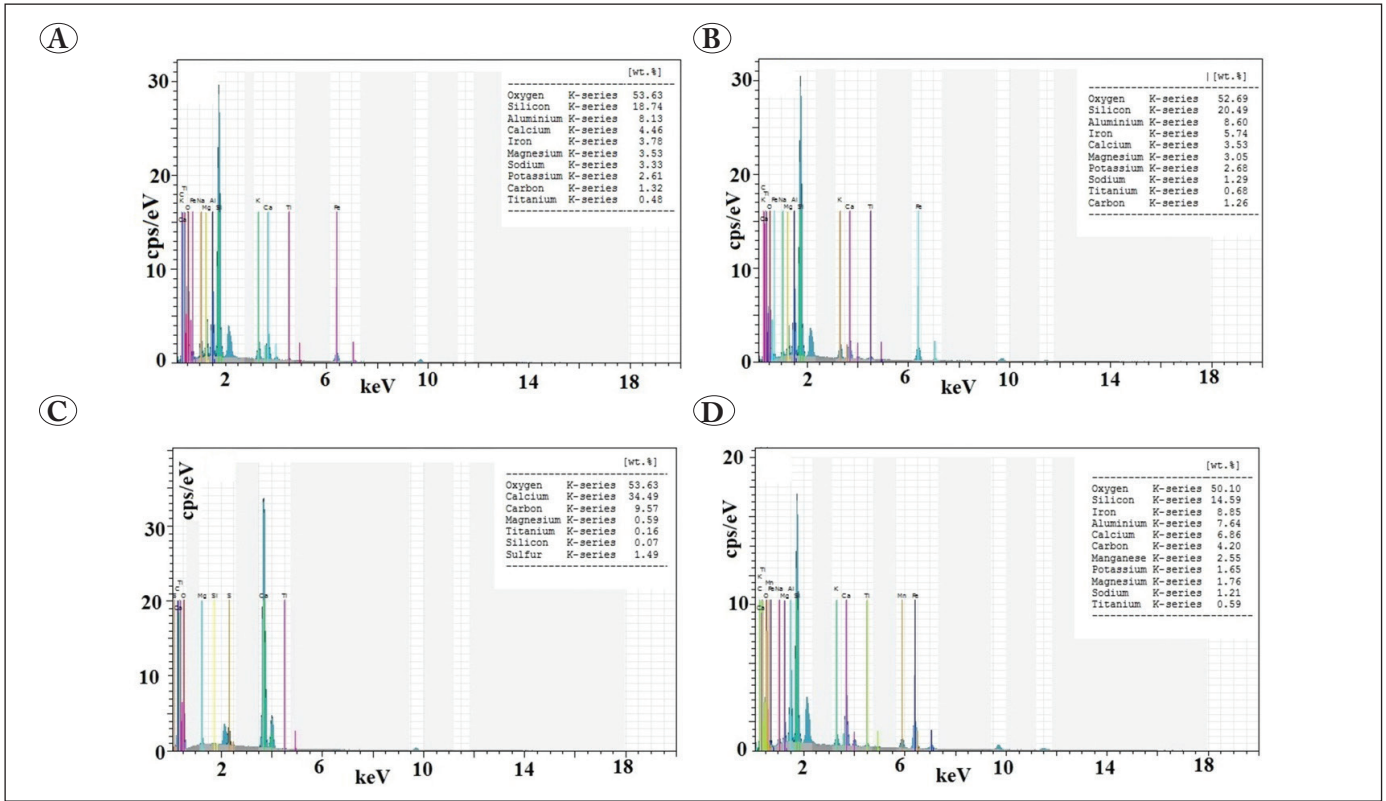


Figure 7. Room temperature EDS results of A) green clay B) red clay C) marble dust D) waste tire.

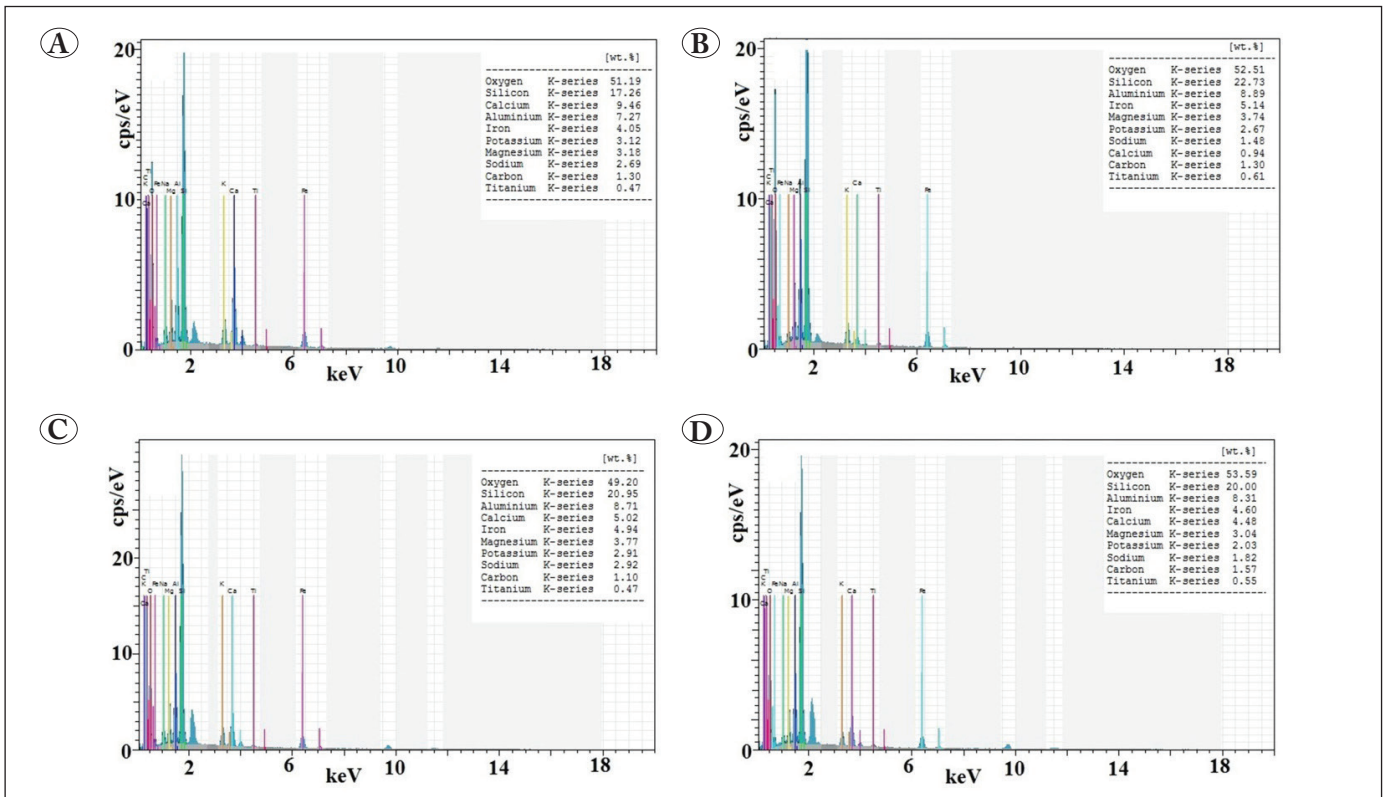
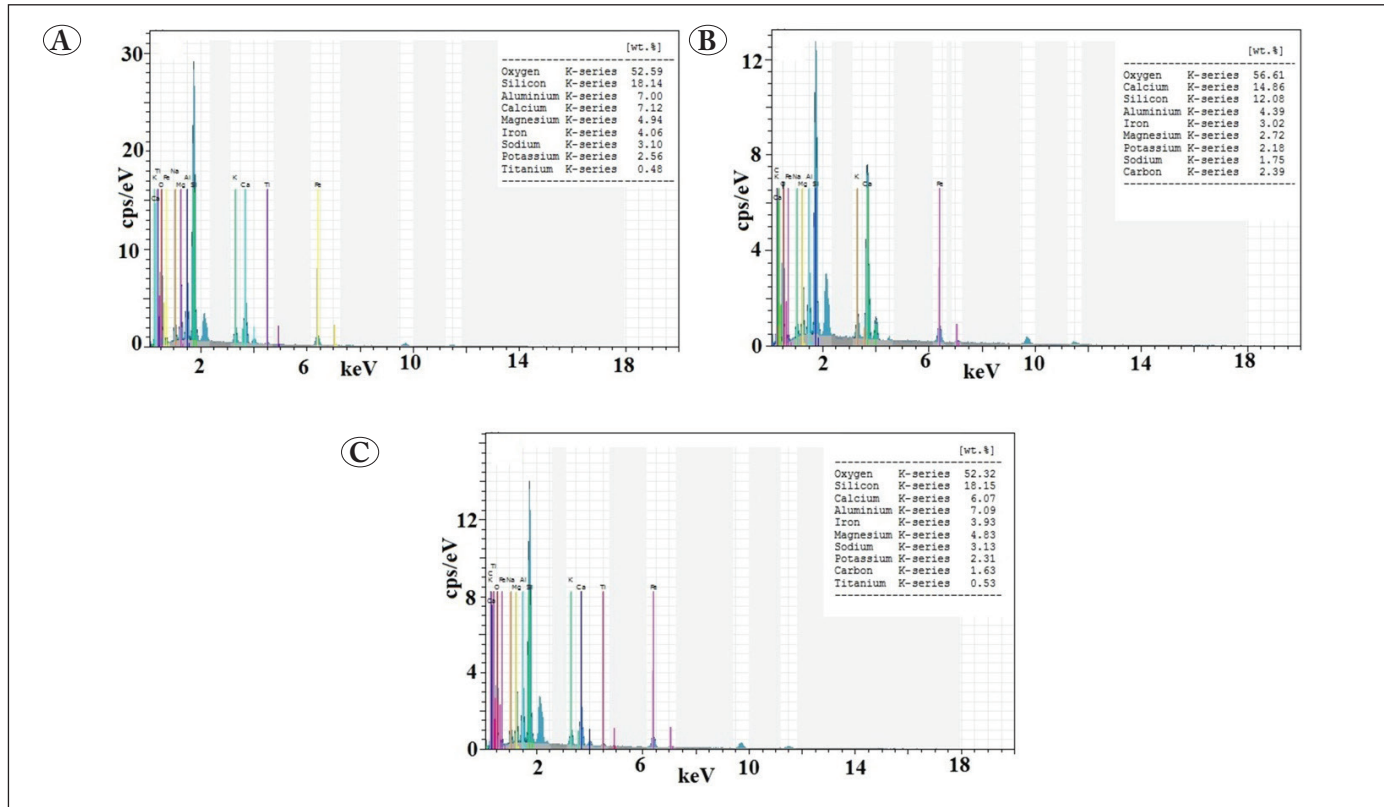


Figure 8. Room temperature EDS results A) green clay with %5 marble dust and %0.5 waste tire B) red clay with %5 marble dust and %0.5 waste tire C) green clay with %5 marble dust D) red clay with %5 marble dust.



**Figure 9.** Room temperature EDS results **A)** silty sand **B)** silty sand with %10 marble dust and %0.5 waste tire **C)** silty sand with %10 marble dust.

(topography), back-scattered electrons (BSE, elastic scattering) are important for analyzing sample composition (Aygun 2013). SEM pictures of all samples have been recorded at room temperature and given in Figures 10-12. Microstructure properties and microcrystalline structures are seen from micrographs.

#### 4. Conclusions

In this paper, clay types and silty sand samples from Oltu/Erzurum region reinforced with reinforcement materials (waste tire and marble dust) have been studied by using spectroscopic techniques in order to see the magnetic and structural properties. Except for marble dust, waste tire and green clay+marble dust samples, for all samples we have obtained an EPR singlet corresponds to  $Fe^{3+}$  ion and  $Mn^{2+}$  sextet lines with forbidden transitions in EPR spectra. EPR spectrum for waste tire gives us a signal with  $g=2.002$  attributed to  $Mn^{4+}$  as a different property that was not seen

in other samples. For all investigated materials, we are able to see the paramagnetic feature. But there is no observed significant difference between unreinforced and reinforced samples. With the help of SEM images, we are able to see the surface features and morphology of the specimens. All kinds of samples have shown microcrystalline property. EDS results gives us the elemental compositions of the samples. This data is in good agreement with the other experimental results in limitations of device sensitivity. From XRD patterns, it is concluded that the crystalline structure of all samples is observed with sharp and intense peaks. These coherent results of the spectroscopic methods give us chance to make a comprehensive analysis of these unreinforced-reinforced materials which can be used in different reinforcement and construction applications. Thus, with the help of these results, the lack of literature about the regional samples are fulfilled.

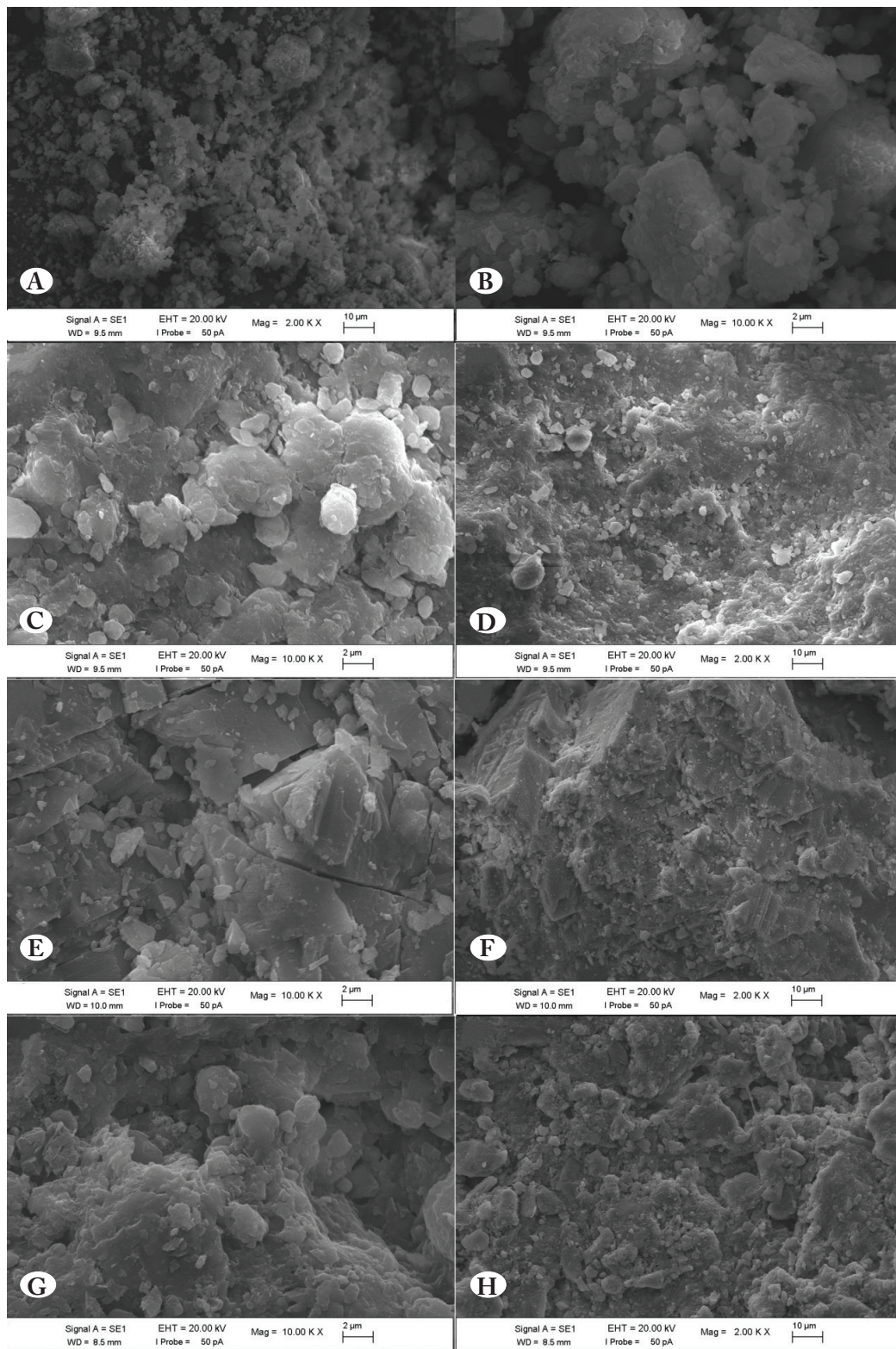


**Figure 10.** Room temperature SEM images of A-B) green clay C-D) red clay E-F) marble dust G-H) waste tire.

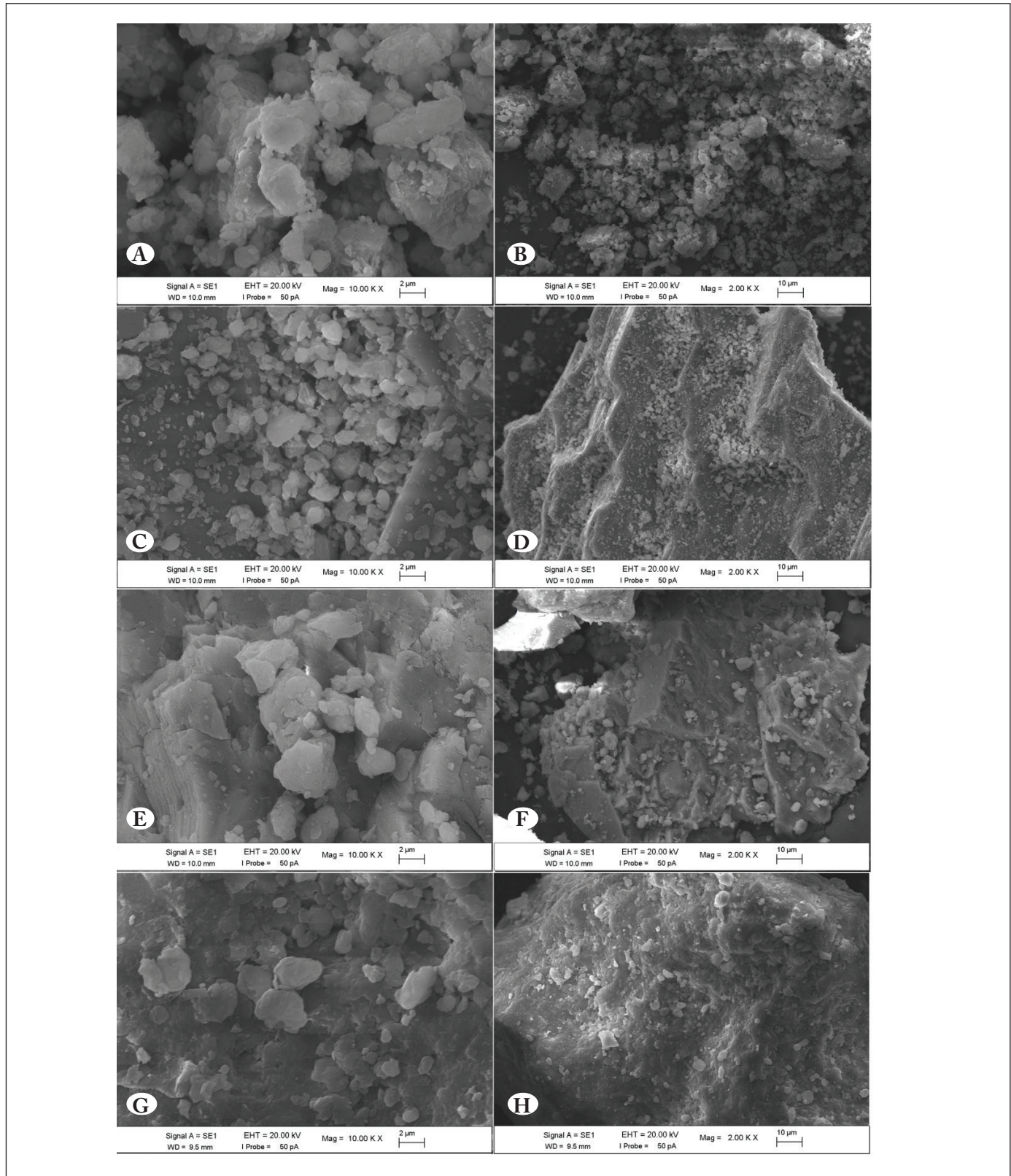


**Figure 11.** Room temperature SEM images **A-B)** green clay with %5 marble dust and %0.5 waste tire **C-D)** red clay with %5 marble dust and %0.5 waste tire **E-F)** green clay with %5 marble dust **G-H)** red clay with %5 marble dust.

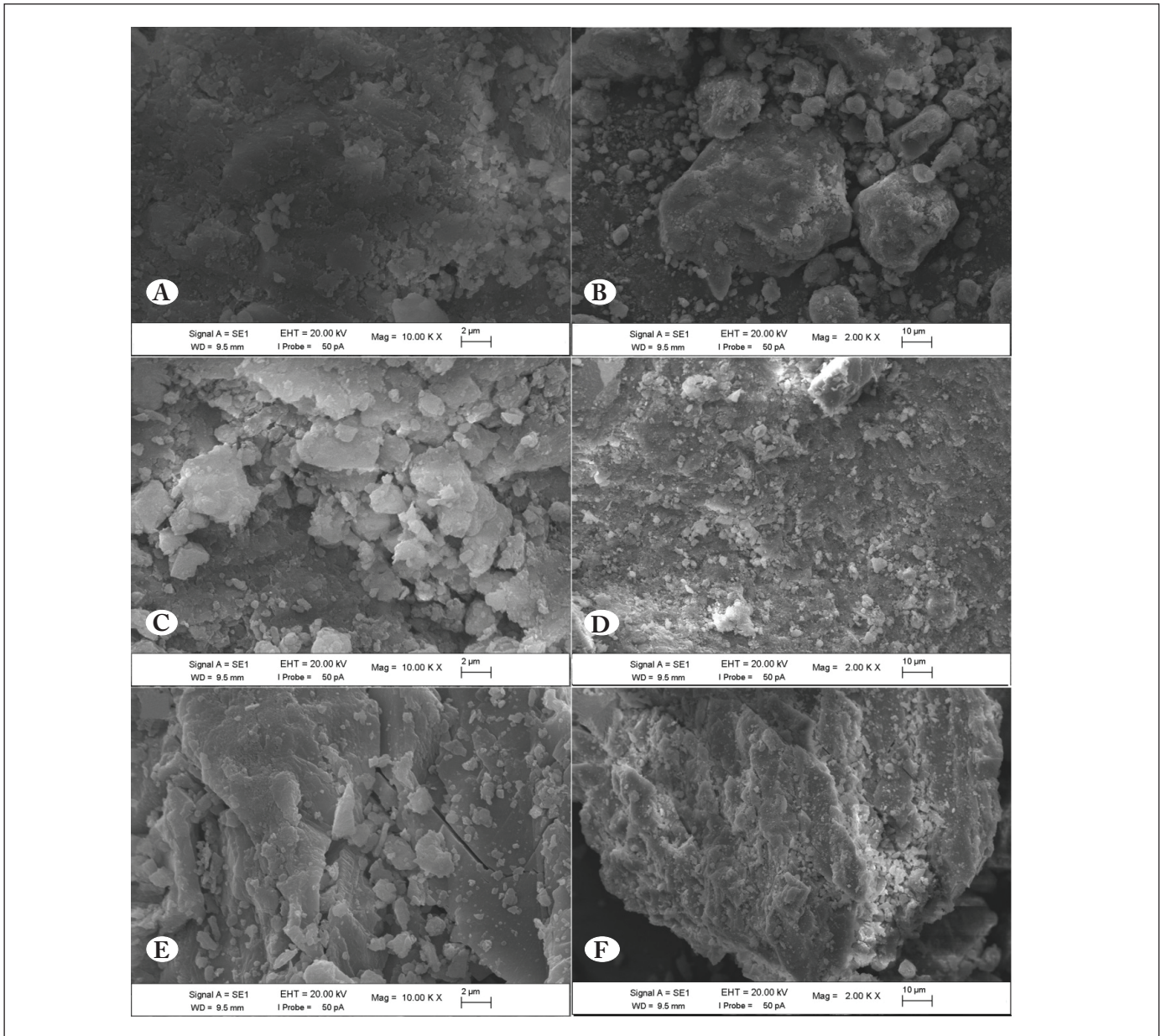


**Figure 12.** Room temperature SEM images of A-B) silty sand C-D) silty sand with %10 marble dust and %0.5 waste tire E-F) silty sand with %10 marble dust.

## 5. References

- Akbulut, S., Arasan, S., Kalkan, E. 2007. Modification of clayey soils using scrap tire rubber and synthetic fibers. *Appl. Clay Sci.*, 38: 23-32.
- Altun, S., Sezer, A., Erol, A. 2009. The effects of additives and curing conditions on the mechanical behavior of a silty soil. *Cold Regions Sci. Tech.*, 56: 135-140.
- Aygun, Z. 2013. AFM and SEM Studies of VO<sub>2</sub><sup>+</sup> Doped Potassium Dihydrogen Citrate Single Crystal Obtained by Slow Evaporation Method. *J. Chem. Crystall.*, 43: 103-107.
- Aygun, Z., Aygun, M. 2016. Spectroscopic analysis of Ahlat stone (ignimbrite) and pumice formed by volcanic activity. *Spectrochim. Acta A*, 166: 73-78.
- Bennur, TH., Srinivasan, D., Ratnasamy, P. 2001. EPR spectroscopy of copper and manganese complexes encapsulated in zeolites. *Microporous Mesoporous Mater.* 48: 111-118.
- Cubitt, JM. 1979. The Geochemistry, Mineralogy and Petrology of Upper Paleozoic Shales of Kansas. *As Kansas Geological Survey Bulletin* 217.

- Ferreira, CS., Santos, PL., Bonacin, JA., Passos, RR., Pocrifk, LA. 2015.** Rice Husk Reuse in the Preparation of SnO<sub>2</sub>/SiO<sub>2</sub> Nanocomposite. *Mater. Res.*, 3: 639-643.
- Fisli, A., Yuni, R., Krisnandi, K., Gunlazuardi, J. 2017.** Preparation and characterization of Fe<sub>3</sub>O<sub>4</sub>/SiO<sub>2</sub>/TiO<sub>2</sub> composite for methylene blue removal in water. *Inter. J. Tech.*, 1: 76-84.
- Ghazavi, M., Roustaei, M. 2010.** The influence of freeze-thaw cycles on the unconfined compressive strength of fiber-reinforced clay. *Cold Regions Sci. Tech.* 61: 125-131.
- Jafari, M., Esna-ashari, M. 2012.** Effect of waste tire cord reinforcement on unconfined compressive strength of lime stabilized clayey soil under freeze-thaw condition. *Cold Regions Sci. Tech.*, 82: 21-29.
- Kalkan, E., Bayraktutan, MS. 2008.** Geotechnical evaluation of Turkish clay deposits: a case study in Northern Turkey. *Environ. Geo.*, 55: 937-950.
- Li, J., Hu, Y., Sun, W., Luo, Y., Shi, X. et al. 2016.** Facile preparation of hyaluronic acid-modified Fe<sub>3</sub>O<sub>4</sub>@Mn<sub>3</sub>O<sub>4</sub> nanocomposites for targeted T<sub>1</sub>/T<sub>2</sub> dual-mode MR imaging of cancer cells. *Royal Soc. Chem.*, 6: 35295-35304.
- Lu, X., Zhang, H., Guo, Y., Wang, Y., Ge, X. et al. 2011.** Hexagonal hydroxyapatite formation on TiO<sub>2</sub> nanotubes under urea modulation. *Cryst. Engineer. Commun.*, 13: 3741-3749.
- Marfunin, AS. 1964.** Radiospectroscopy of minerals. *Geo. J.*, 4: 361-390.
- Musolino, M.G., Busacca, C., Mauriello, F., Pietropaolo, R. 2010.** Aliphatic carbonyl reduction promoted by palladium catalysts under mild conditions. *Appl. Catalysis A*, 379: 77-86.
- Rahman, M.A., Halfar, J., Shinjo, R. 2013.** X-Ray Diffraction Is a Promising Tool to Characterize Coral Skeletons. *Advan. Mater. Phys. Chem.*, 3: 120-125.
- Senderowski, C. 2014.** Nanocomposite Fe-Al Intermetallic Coating Obtained by Gas Detonation Spraying of Milled Self-Decomposing Powder. *J. Thermal Spray Tech.*, 7: 1124-1134.
- Shu, Z., Wang, S. 2009.** Synthesis and Characterization of Magnetic Nanosized Fe<sub>3</sub>O<sub>4</sub>/MnO<sub>2</sub> Composite Particles. *J. Nanomater.*, 1-5.
- Stoyanova, R., Gorova, M., Zhecheva, E. 2000.** EPR monitoring of Mn<sup>4+</sup> distribution in Li<sub>4</sub>Mn<sub>5</sub>O<sub>12</sub> spinels. *J. Phys. Chem. Solids*, 61: 615-620.
- Sun, M., Lan, B., Lin, T., Cheng, G., Ye, F. et al. 2013.** Controlled synthesis of nanostructured manganese oxide: crystalline evolution and catalytic activities. *Cryst. Engineer. Commun.*, 15: 7010-7018.
- Taşpolat, LT., Zorluer, İ., Koyuncu, H. 2006.** Atik mermer tozunun geçirimsiz kil tabakalarda donma - çözölmeye etkisi. *Yapı Teknolojileri Elektronik Dergisi*, 2: 11-16.
- Wei, H., Jiao, Y., Liu, H. 2015.** Effect of freeze-thaw cycles on mechanical property of silty clay modified by fly ash and crumb rubber. *Cold Regions Sci. Techn.*, 116: 70-77.
- Yang, S., Cai, W., Zeng, H., Xu, X. 2009.** Ultra-fine β-SiC quantum dots fabricated by laser ablation in reactive liquid at room temperature and their violet emission. *J. Mater. Chem.*, 19: 7119-7123.
- Yarbasi, Z., Karabulut, B., Karabulut, A. 2011.** An EPR Study of Gamma Irradiated Medicinal Plants: Cress Seeds and Mistletoe. *Gazi Univ. J. Sci.*, 2: 203-207.
- Yarbaşı, N. (2016)** Geotechnical mapping of Oltu (Erzurum) residential area and its vicinity. *Pamukkale Univ. J. Engineer. Sci.*, 22: 538-545.
- Zhang, W., Zeng, Y., Xu, C., Xiao, N., Gao, Y. 2012.** A facile approach to nanoarchitected three-dimensional graphene-based Li-Mn-O composite as high-power cathodes for Li-ion batteries. *Beilstein J. Nanotech.*, 3: 513-523.